JACS
JOURNAL OF THE AMERICAN CHEMICAL SOCIETY

Article

pubs.acs.org/JACS

Fluorescent Charge-Assisted Halogen-Bonding Macrocyclic Halo-Imidazolium Receptors for Anion Recognition and Sensing in Aqueous Media

Fabiola Zapata,[†] Antonio Caballero,[†] Nicholas G. White,[†] Tim D. W. Claridge,[†] Paulo J. Costa,[‡] Vítor Félix,[‡] and Paul D. Beer*[,†]

[†]Chemistry Research Laboratory, Department of Chemistry, University of Oxford, Mansfield Road, Oxford OX1 3TA, U.K.

[‡]Departamento de Química, CICECO and Secção Autónoma de Ciências da Saúde, Universidade de Aveiro, 3810-193 Aveiro, Portugal

Supporting Information

ABSTRACT: The synthesis and anion binding properties of a new family of fluorescent halogen bonding (XB) macrocyclic halo-imidazolium receptors are described. The receptors contain chloro-, bromo-, and iodo-imidazolium motifs incorporated into a cyclic structure using naphthalene spacer groups. The large size of the iodine atom substituents resulted in the isolation of anti and syn conformers of the iodo-imidazoliophane, whereas the chloro- and bromo-imidazoliophane analogues exhibit solution dynamic conformational behavior. The syn iodo-imidazoliophane isomer forms novel dimeric isostructural XB complexes of 2:2 stoichiometry with bromide and iodide anions in the solid state. Solution phase DOSY NMR experiments indicate iodide recognition takes place via cooperative convergent XB−iodide 1:1 stoichiometric binding in aqueous solvent mixtures. ^{1}H NMR and fluorescence spectroscopic titration experiments with a variety of anions in the competitive CD_3OD/D_2O (9:1) aqueous solvent mixture demonstrated the bromo- and syn iodo-imidazoliophane XB receptors to bind selectively iodide and bromide respectively, and sense these halide anions exclusively via a fluorescence response. The protic-, chloro-, and anti iodo-imidazoliophane receptors proved to be ineffectual anion complexants in this aqueous methanolic solvent mixture. Computational DFT and molecular dynamics simulations corroborate the experimental observations that bromo- and syn iodo-imidazoliophane XB receptors form stable cooperative convergent XB associations with bromide and iodide.

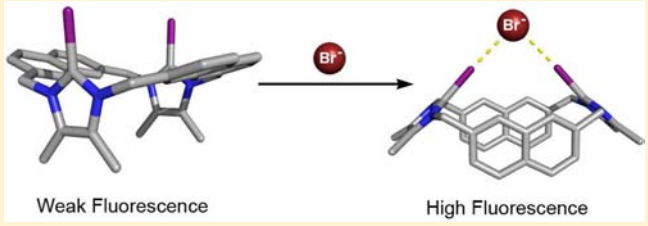

1. INTRODUCTION

Inspired by the many fundamental roles negatively charged species play in a range of chemical, biological, medical, and environmental processes, the field of anion supramolecular chemistry has expanded enormously during the past few decades.[1] Through the imaginative manipulation of a variety of complementary noncovalent interactions such as electrostatics, hydrogen bonding, Lewis acid−base,[2] and anion−π interactions,[3] numerous efficient synthetic anion receptors have been developed. However, the challenge of raising the degree of recognition to that of biotic systems, a requirement for potential commercial exploitation in anion sensing, for example, remains a significant one. Halogen bonding (XB) is the attractive highly directional, intermolecular interaction between electron deficient halogen atoms and Lewis bases[4] which has been exploited successfully in the solid state crystal engineering[5] of liquid crystalline and conductive material[6] design. The complementary analogy to ubiquitous hydrogen bonding has also stimulated the utilization of XB in solution phase molecular recognition processes which is rapidly becoming an established field in its own right.[7] Importantly, the relatively few examples of XB anion receptors reported to date all exhibit promising anion recognition behavior in competitive polar and polar/aqueous solvent media.[8] In addition, the combination of cooperative halogen and hydrogen bonding in urea-based[9] and interlocked rotaxane anion receptors has been shown to modulate anion binding selectivity.[10] With the objective of constructing the first examples of fluorescent XB chemosensors for anions capable of operating in aqueous solvent mixtures,[11] we describe herein the synthesis of a series of novel charge-assisted bidentate chloro-, bromo-, and iodo-imidazoliophane receptors which incorporate fluorescent naphthalene antenna groups into their macrocyclic host frameworks. NMR and fluorescence spectroscopic investigations, together with X-ray structural determinations and computational DFT and molecular dynamics simulations, demonstrate the remarkable ability of the bromo- and iodo-imidazoliophane XB receptors to selectively sense iodide and bromide anions, respectively, in competitive aqueous/methanol media.

Received: March 6, 2012
Published: June 16, 2012

dx.doi.org/10.1021/ja302213r | J. Am. Chem. Soc. 2012, 134, 11533−11541

2. RESULTS AND DISCUSSION

2.1. Synthetic Strategy. The novel bidentate haloimidazoliophane receptors were prepared by a stepwise procedure involving the initial synthesis of bis(2-haloimidazolylmethyl)-naphthalene derivatives (**3b**−**3d**). Reaction of equimolar mixtures of **3b**−**3d** and **1** gave respective haloimidazoliophane bromide salt cyclic products. Importantly, whereas with the chloro- and bromo-imidazoliophanes, only one respective conformer, $\mathbf{5}^{2+}\cdot 2Br^-$ and $\mathbf{6}^{2+}\cdot 2Br^-$, was isolated, two product iodo-imidazoliophane conformers, anti $\mathbf{7}^{2+}\cdot 2Br^-$ and syn $\mathbf{8}^{2+}\cdot 2Br^-$, were separated by repeated recrystallization from methanol. The steric demands of the larger iodine atom imidazolium substituents inhibit intramolecular ring rotation, which results in the isolation of the two conformers in the isomer ratio of anti/syn 35:65. Anion exchange to the corresponding hexafluorophosphate salts was achieved on addition of aqueous NH_4PF_6. The protic imidazoliophane receptor $\mathbf{4}^{2+}\cdot 2PF_6^-$ was synthesized following an analogous procedure using 4,5-dimethyl-1*H*-imidazole (**2a**) as the starting material (Scheme 1).

Scheme 1. Synthesis of Macrocyclic Receptors $\mathbf{4}\cdot(PF_6)_2$−$\mathbf{8}\cdot(PF_6)_2$[a]

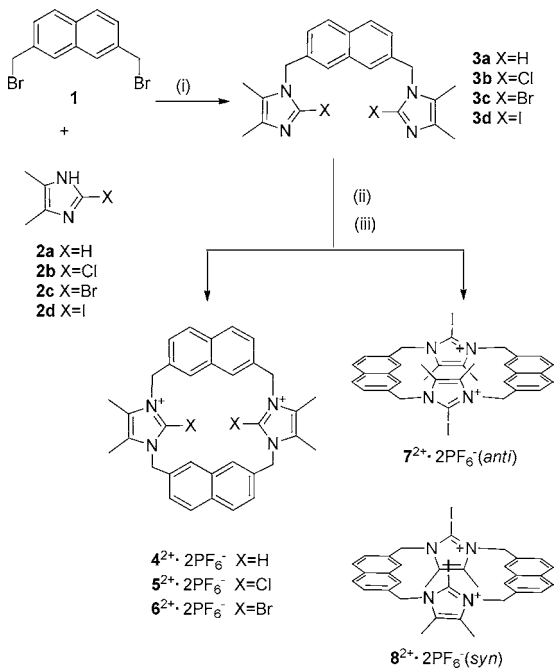

[a]Reagents and conditions: (i) NaOH (1 M in water), CH_3CN, reflux, **3a**, 70%; **3b**, 58%; **3c**, 65%; **3d**, 68%; (ii) 2,7-bis(bromomethyl)-naphthalene, CH_3CN, reflux; (iii) wash with saturated NH_4PF_6 (aq), $\mathbf{4}\cdot(PF_6)_2$, 75%; $\mathbf{5}\cdot(PF_6)_2$, 45%; $\mathbf{6}\cdot(PF_6)_2$, 70%; $\mathbf{7}\cdot(PF_6)_2$, 23%; $\mathbf{8}\cdot(PF_6)_2$, 44%.

2.2. Studies of Conformers in Solution. Xylyl-linked imidazolium and benzimidazolium cyclophanes have been demonstrated to exhibit fluxional behavior in solution via the interconversion of different conformers.[12] It was of interest therefore to investigate the solution dynamic conformational properties of the bidentate haloimidazoliophane receptors by variable temperature ^{1}H NMR in DMSO-d_6 solution. The room-temperature ^{1}H NMR spectra of the protic imidazoliophane receptor $\mathbf{4}^{2+}\cdot 2PF_6^-$ revealed a sharp singlet for the methylene protons (δ = 5.72 ppm) and singlets for the methyl groups (δ = 2.08 ppm) and the C−H protons of the imidazolium ring (δ = 9.31 ppm) which indicates rapid interconversion of all possible conformations on the NMR time scale. By contrast, the ^{1}H NMR spectra at room temperature of receptors $\mathbf{5}^{2+}\cdot 2PF_6^-$ and $\mathbf{6}^{2+}\cdot 2PF_6^-$ exhibited several signals for the methylene and methyl protons, attributed to the presence of different conformers in solution. The ratio between the anti and syn isomers was 28:72 in the case of the receptor $\mathbf{5}^{2+}\cdot 2PF_6^-$ and 25:75 for the receptor $\mathbf{6}^{2+}\cdot 2PF_6^-$. On warming a DMSO-$d_6$ solution of chloroimidazoliophane $\mathbf{5}^{2+}\cdot 2PF_6^-$, the signals began to broaden and finally coalesced to one signal at 100 °C, suggesting rapid interconversion of the different conformations on the NMR time scale. The rate constant and the free energy of activation for the anti → syn exchange process were calculated[13] from the variable-temperature NMR data to be 86 s^{-1} at 100 °C and 78 kJmol^{-1}, respectively (Figure 1).

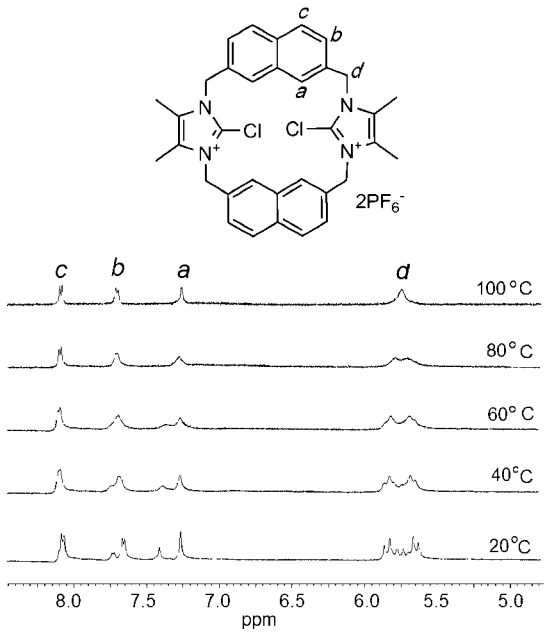

Figure 1. Variable-temperature ^{1}H NMR spectra (aromatic region) in DMSO-d_6 of receptor $\mathbf{5}^{2+}\cdot 2PF_6^-$.

The bromoimidazoliophane $\mathbf{6}^{2+}\cdot 2PF_6^-$ exhibited similar VT ^{1}H NMR behavior to that of $\mathbf{5}^{2+}\cdot 2PF_6^-$ with a room temperature conformational ratio of anti/syn 25:75 and a higher coalescence temperature (120 °C) (see Supporting Information). The determined rate constant at coalescence (41 s^{-1}) and free energy of activation energy (85 kJmol^{-1}) suggests the conformational anti → syn interconversion for $\mathbf{6}^{2+}\cdot 2PF_6^-$ is more energetically difficult than the conformer exchange process for the chloroimidazoliophane receptor, as might be expected due to the former receptor's larger sized bromine atoms.

An analogous VT ^{1}H NMR study with anti and syn iodoimidazoliophane receptors $\mathbf{7}^{2+}\cdot 2PF_6^-$ and $\mathbf{8}^{2+}\cdot 2PF_6^-$ revealed no changes in the respective ^{1}H NMR spectra. Presumably, the steric demands of the iodine atom imidazolium substituents completely inhibit intramolecular ring rotation, which results in the isolation of the two conformers. The ^{1}H NMR spectra of the iodoimidazoliophanes $\mathbf{7}^{2+}\cdot 2PF_6^-$ (anti) and $\mathbf{8}^{2+}\cdot 2PF_6^-$ (syn) are very similar with only slight differences in some chemical shift values being observed.

dx.doi.org/10.1021/ja302213r | J. Am. Chem. Soc. 2012, 134, 11533−11541

2.3. X-ray Crystallography. Crystals suitable for single crystal X-ray diffraction structural analysis were obtained of the bis-hexafluorophosphate salt of 7^{2+}, and of the mixed hexafluorophosphate-bromide and hexafluorophosphate-iodide salts of 8^{2+}. The latter two complexes are isostructural in the solid state, both crystallizing in the unusual cubic space group, $Im\bar{3}$.

In the structures that contain hexafluorophosphate anions, no XB is observed between these anions and the haloimidazolium cations (Figure 2).

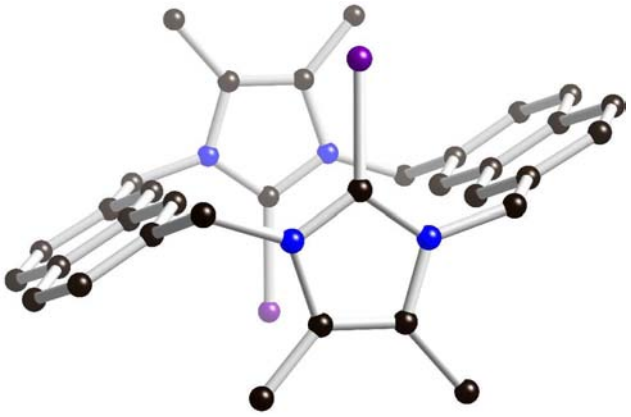

Figure 2. Ball and stick model of the X-ray crystal structure of $7^{2+}\cdot 2PF_6^-$; hexafluorophosphate counteranions and hydrogen atoms are omitted for clarity. Color scheme: gray = carbon, blue = nitrogen, purple = iodine.

The larger size of the naphthalene-containing macrocycles allows for a dimeric arrangement in the solid state whereby two macrocycles surround two halide anions in a pincer-like arrangement (Figures 3 and 4).

Details of XB in the solid state are summarized in Table 1. Two clear trends are observed: first, a XB interaction causes a significant increase in the haloimidiazolium C-halide bond length compared with this bond length in the corresponding bis-hexafluorophosphate compound. This is consistent with a weakening of the C–X bond (X = halogen substituent of the imidazolium motif) due to electron donation from the anion into the C–X σ^* orbital.[14]

For the structures where the anion is bromide, the X···Br distance *decreases* with increasing size of X. This then results in a large drop in the percentage of the sum of the van der Waals (VdW) radii from 86 to 87% when X = Br, to 81% when X = I. This is consistent with increasing halogen bonding strength when a larger, more polarizable halogen is used as the Lewis acid. Interestingly, however, when iodide is used as the anion instead of bromide, the halogen bond length *increases* as does the percentage of VdW radii suggesting a weaker halogen bond, consistent with the solution binding studies (vide infra), and our previous results on a bromo-imidazoliophane xylene system.[8a] The XB angles are close to linear which is typical of such systems.[8a,g,h]

2.4. Anion Binding Studies. The anion binding properties of the receptors were investigated initially by ^{1}H NMR titration experiments with various tetrabutylammonium (TBA^+) anion salts (F^-, Cl^-, Br^-, I^-, NO_3^-, $H_2PO_4^-$, SO_4^{2-}, $C_6H_5{-}COO^-$ and AcO^-) in the competitive aqueous solvent mixture CD_3OD/D_2O 9:1.

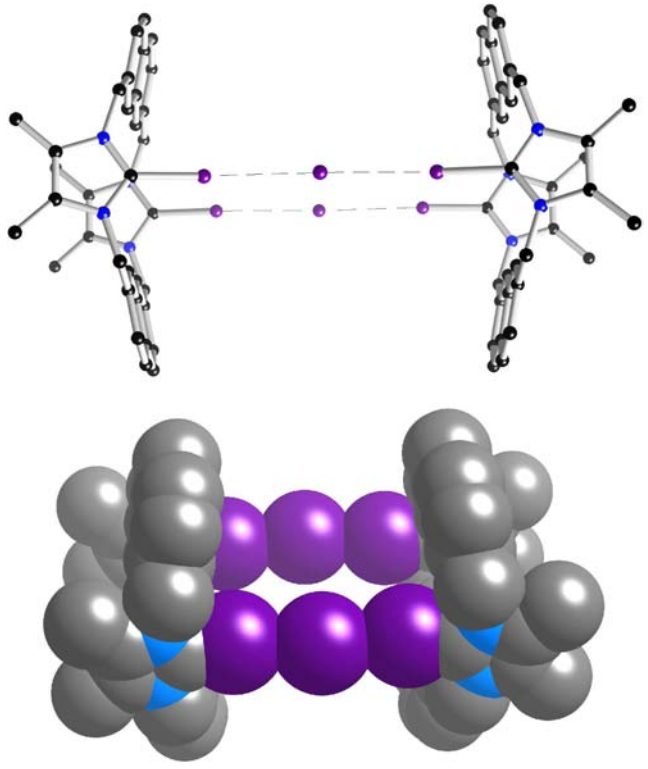

Figure 3. Ball and stick representation (top) and space-filling packing (bottom) of the solid-state structure of $8^{2+}\cdot I^-\cdot PF_6^-$; hexafluorophosphate anions and hydrogen atoms are omitted for clarity. Color scheme: gray = carbon, blue = nitrogen, purple = iodine.

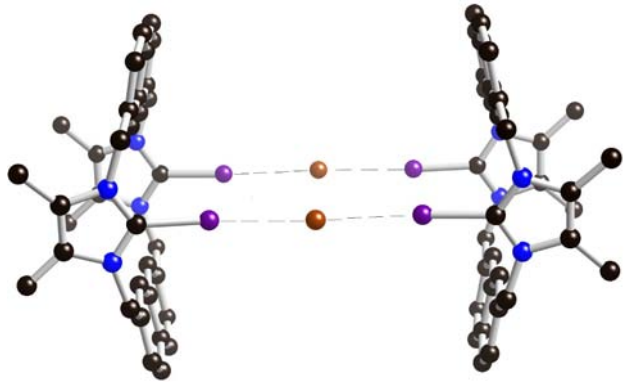

Figure 4. Ball and stick model of the X-ray crystal structure of $8^{2+}\cdot Br^-\cdot PF_6^-$. Halogen bonds are shown as dashed lines, hexafluorophosphate anions are omitted for clarity. Color scheme: gray = carbon, blue = nitrogen, purple = iodine, orange = bromide. This structure is isostructural with $8^{2+}\cdot I^-\cdot PF_6^-$.

Table 1. Details of Halogen Bonding in the Solid State

compound, C–X substituent (conformer)	C–X [Å][a]	C–X···Br [Å]	X···Br [%][b]	∠C–X···Br (deg)
$8^{2+}\cdot Br^-\cdot PF_6^-$ (syn)	2.094(8)	3.095(1)	81	167.48(19)
compound, C–X substituent (conformer)	C–X [Å][a]	C–X···I [Å]	X···I [%][b]	∠C–X···I (deg)
$8^{2+}\cdot I^-\cdot PF_6^-$ (syn)	2.079(6)	3.303(1)	83	167.90(14)

[a]C–X in corresponding PF_6 salt. [b][%] of VdW radii.

It is noteworthy that addition of a large excess of the TBA^+ anion salts to receptors $5^{2+}\cdot 2PF_6^-$ and $7^{2+}\cdot 2PF_6^-$ (anti) caused

dx.doi.org/10.1021/ja302213r | J. Am. Chem. Soc. 2012, 134, 11533–11541

no significant changes in the ^{1}H NMR spectra, whereas significant perturbations were only observed with receptors $\mathbf{6}^{2+}\cdot 2PF_6^-$ and $\mathbf{8}^{2+}\cdot 2PF_6^-$ (syn) upon addition of bromide and iodide anions. As might be expected in this competitive aqueous methanolic solvent media, the chloroimidazolium receptor $\mathbf{5}^{2+}\cdot 2PF_6^-$ is an ineffectual anion complexing regent due to the chlorine atom being a relatively poor XB donor.[7s] In the case of the anti iodo-imidazoliophane isomer $\mathbf{7}^{2+}\cdot 2PF_6^-$, these NMR observations suggest a single charge assisted XB interaction is unable to bind anions in this protic media.

At room-temperature in CD_3OD/D_2O 9:1, the ^{1}H NMR spectrum of $\mathbf{6}^{2+}\cdot 2PF_6^-$ displays an anti/syn conformer ratio of 25:75. Addition of increasing amounts of Br^- anions induced significant downfield shifts of the internal naphthalene protons ($\Delta\delta$ = 0.19 ppm), concomitant with a change in the ratio of conformers to 8:92 anti/syn after addition of 2 equiv of bromide (see Supporting Information). Addition of I^- anion caused similar chemical shift changes, where a larger magnitude of perturbation for the naphthalene protons ($\Delta\delta$ = 0.40 ppm) was observed. Importantly, in the presence of 2 equiv of I^-, the syn conformer dominates (2:98, anti/syn) (Figure 5).

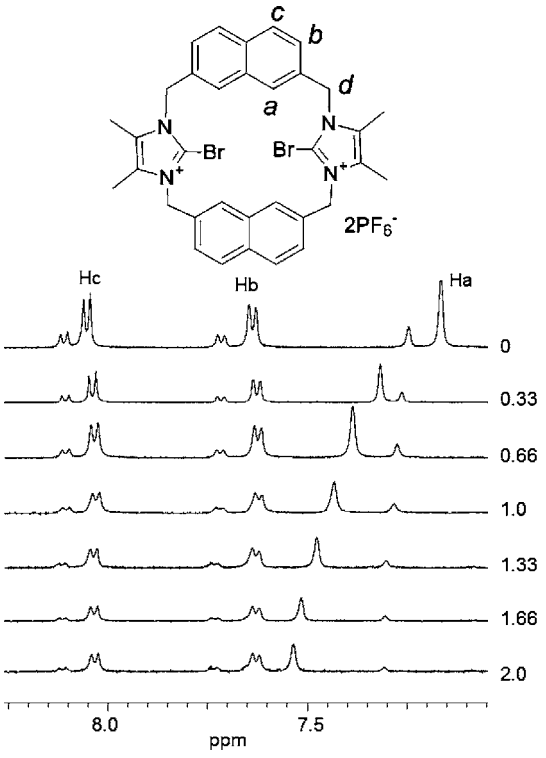

Figure 5. ^{1}H NMR spectral changes observed in the aromatic region of $\mathbf{6}^{2+}\cdot 2PF_6^-$, in CD_3OD/D_2O 9:1 at 20 °C during the addition of up to 2 equiv of iodide ions.

Monitoring the naphthalene proton *a* of receptor $\mathbf{6}^{2+}\cdot 2PF_6^-$, WinEQNMR analysis[15] of the titration data revealed the receptor binds bromide and iodide anions very strongly, beyond the limits of the NMR technique ($K_a > 1 \times 10^4$ M^{-1}).

In a similar fashion, addition of Br^- and I^- anions to a solution of $\mathbf{8}^{2+}\cdot 2PF_6^-$ (syn) receptor in CD_3OD/D_2O 9:1 induced downfield shifts of the internal naphthalene protons, $\Delta\delta$ = 0.08 ppm for bromide and $\Delta\delta$ = 0.23 ppm for iodide (Figure 6).

Job–plot analysis revealed both receptors to form 1:1 stoichiometric complexes with Br^- and I^- anions. To ascertain

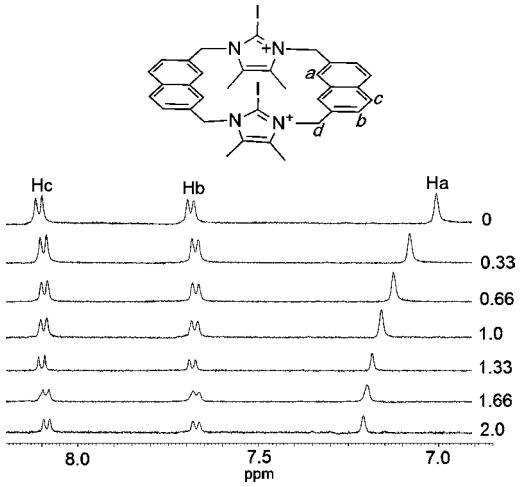

Figure 6. ^{1}H NMR spectral changes observed in the aromatic region of $\mathbf{8}^{2+}\cdot 2PF_6^-$ (syn) in CD_3OD/D_2O 9:1 at 20 °C during the addition of up to 2 equiv of iodide ions.

whether the halide recognition phenomenon in solution was dimeric in nature, as suggested by the crystal structure of $\mathbf{8}^{2+}\cdot I^-\cdot PF_6^-$ (Figure 3), DOSY NMR spectroscopic experiments were carried out in a solution of a ~2:1 syn/anti mixture of $\mathbf{8}^{2+}\cdot 2PF_6^-$ and $\mathbf{7}^{2+}\cdot 2PF_6^-$ with 0, 6, and 10 equiv of NBu_4I in DMSO-d_6/D_2O 9:1[16] (see Supporting Information for experimental details). Dimeric association in solution should result in a decrease in diffusion coefficient for the syn isomer only as I^- is added, whereas the anti isomer would be expected to show little or no reduction as it would be unable to form such a dimeric complex. To account for potential variations in solution viscosity on addition of NBu_4I, the diffusion coefficients were normalized to that of the solvent DMSO. The diffusion data for both the syn and anti complexes (Table 2) show no significant change on addition of increasing amounts of I^- with any small variation being attributable to viscosity changes (as evidenced by the normalized $D_{complex}/D_{solvent}$ ratios) and suggests the dimeric structure does not exist as a stable entity in solution under these conditions. Experiments employing greater excesses of I^- were not possible owing to sample precipitation.

It was not possible to determine association constant values with bromide and iodide halide ions with receptor $\mathbf{8}^{2+}\cdot 2PF_6^-$ due to complex precipitation during the titration experiments. With the protic macrocycle $\mathbf{4}^{2+}\cdot 2PF_6^-$ the C-*H* proton of the imidazolium ring, which in the free receptor appears at δ = 9.31 ppm, shifted downfield upon the addition of chloride ($\Delta\delta$ = 0.09 ppm), and bromide and iodide ions ($\Delta\delta$ = 0.10 ppm). Significant downfield perturbations were also noted in the internal naphthalene protons upon halide anion addition (chloride $\Delta\delta$ = 0.09 ppm; bromide $\Delta\delta$ = 0.11 ppm; iodide $\Delta\delta$ = 0.17 ppm).

Association constants for 1:1 stoichiometric halide anion binding were determined by WinEQNMR[16] analysis of the titration data, monitoring the internal aromatic protons of receptor $\mathbf{4}^{2+}\cdot 2PF_6^-$. The association constant values for chloride, bromide, and iodide anions of K_a (error) = 19 (1), 85 (1), and 80 (3) M^{-1}, respectively, indicate the protic receptor binds the halides weakly in this competitive aqueous methanolic solvent mixture.[17]

By virtue of the naphthalene groups present in the cyclophane receptors, fluorescence spectroscopy was used to

dx.doi.org/10.1021/ja302213r | J. Am. Chem. Soc. 2012, 134, 11533–11541

Table 2. NMR Diffusion Coefficients for $8^{2+}\cdot 2PF_6^-$ and $7^{2+}\cdot 2PF_6^-$ in DMSO/D_2O 9:1 at 20 °C in the Absence and Presence of I^- (Added as NBu_4I)[a]

	$8^{2+}\cdot 2PF_6^-$ + $7^{2+}\cdot 2PF_6^-$		$8^{2+}\cdot 2PF_6^-$ + $7^{2+}\cdot 2PF_6^-$ + 6 equiv I^-		$8^{2+}\cdot 2PF_6^-$ + $7^{2+}\cdot 2PF_6^-$ + 10 equiv I^-	
	anti	syn	anti	syn	anti	syn
$D_{complex}/10^{-10}$ m^2 s^{-1}	1.14	1.14	1.18	1.19	1.16	1.17
$D_{solvent}/10^{-10}$ m^2 s^{-1}	4.52		4.73		4.65	
$D_{complex}/D_{solvent}$	0.252	0.252	0.249	0.251	0.249	0.252

[a]D value errors are ±0.01 × 10^{-10} m^2 s^{-1}.

investigate their anion sensing capabilities in CH_3OH/H_2O 9:1. In agreement with the ^{1}H NMR titration results, upon addition of F^-, Cl^-, NO_3^-, $H_2PO_4^-$, SO_4^{2-}, $C_6H_5{-}COO^-$, and AcO^-, no changes in the fluorescence emission spectrum of $6^{2+}\cdot 2PF_6^-$ and $8^{2+}\cdot 2PF_6^-$ (syn) were observed even when in large excess. By contrast, in the presence of Br^- and I^- anions, an increase in emission bands was seen.

The emission spectrum of $6^{2+}\cdot 2PF_6^-$ when excited at λ_{exc} = 355 nm displays a structureless band at 401 nm, and upon addition of equivalents of I^-, two important anion binding induced effects in the fluorescent spectrum were noted: an increase of the intensity of the emission band present in the free ligand at 401 nm, and the appearance of a new emission band at λ_{em}= 437 nm which is accompanied by an increase of the intensity emission (I_{max}/I_o = 5.8) (Figure 7). In the presence of 1.5 equiv of Br^- anion, a smaller increase of the emission band at 437 nm was observed (I_{max}/I_o = 2) (see Supporting Information).

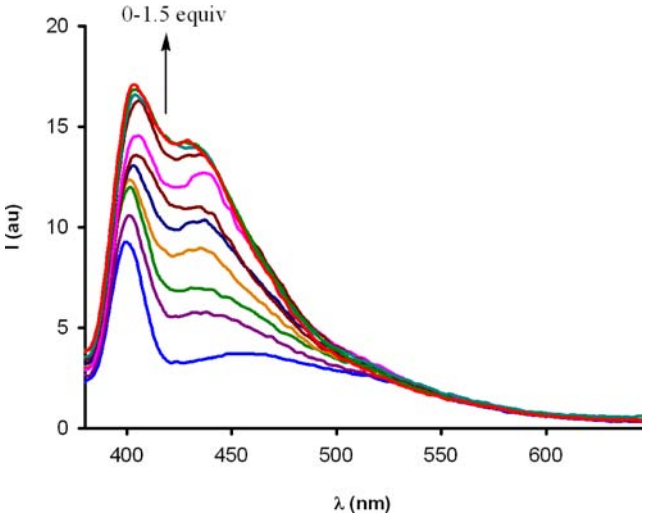

Figure 7. Changes in the fluorescence spectra of receptor $6^{2+}\cdot 2PF_6^-$ (1 × 10^{-5} M) in CH_3OH/H_2O 9:1 upon addition of iodide at 20 °C.

The addition of increasing amounts of Br^- anion to a solution of receptor $8^{2+}\cdot 2PF_6^-$ in the same aqueous solvent mixture induced a red shift of the emission band from 401 to 410 nm ($\Delta\lambda$ = 9 nm) accompanied by a remarkable increase of the intensity of the emission band that appears at λ_{em} = 437 nm (I_{max}/I_o = 6.4) (Figure 8). A relatively smaller emission enhancement was detected when 1.5 equiv of I^- anion was added (I_{max}/I_o = 1.6) (see Supporting Information). Analogous fluorescence spectroscopic anion titration experiments with hydrogen-bonding receptor $4^{2+}\cdot 2PF_6^-$ and the chloroimidazoliophane $5^{2+}\cdot 2PF_6$ produced no significant emission responses with any anion. Specfit[18] analysis of the fluorescent titration

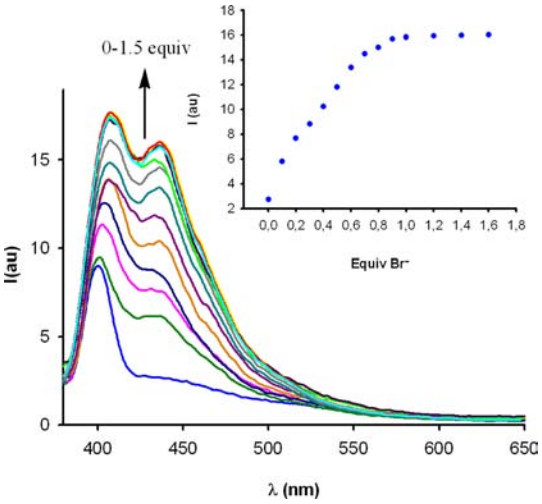

Figure 8. Changes in the fluorescence spectra of receptor $8^{2+}\cdot 2PF_6^-$ (1 × 10^{-5} M) in CH_3OH/H_2O 9:1 upon addition of Br^- ion. Inset: Changes of emission upon addition of Br^- at 20 °C.

data determined 1:1 association constant values for Br^- and I^- binding shown in Table 3.

Table 3. Association Constants K_a for Receptors $6^{2+}\cdot 2PF_6^-$ and $8^{2+}\cdot 2PF_6^-$ with Different Anions in CH_3OH/H_2O 9:1 at 20 °C

	K_a (M^{-1})[b]	
anion[a]	$6^{2+}\cdot 2PF_6^-$	$8^{2+}\cdot 2PF_6^-$
Br^-	2.88 × 10^4	9.55 × 10^5
I^-	6.31 × 10^5	3.71 × 10^4

[a]Anions have been used as tetrabutylammonium salt. [b]Error < 10%.

Both receptors bind Br^- and I^- strongly in this aqueous solvent mixture with the bidentate bromo-imidazoliophane $6^{2+}\cdot 2PF_6^-$ exhibiting selectivity for iodide, whereas the reverse halide preference for bromide is displayed by iodo-imidazoliophane receptor *syn* $8^{2+}\cdot 2PF_6^-$. It is noteworthy that computational DFT and molecular dynamics simulations discussed in the following section corroborate these experimental findings that both XB receptors form strong and stable associations with the heavier halide anions. Thus, these results highlight the fact that the incorporation of bromine and iodine atoms into the bis(imidazolium) naphthalene macrocyclic receptor framework dramatically influences the anion recognition capabilities of the cyclic host, with receptors $6^{2+}\cdot 2PF_6^-$ and $8^{2+}\cdot 2PF_6^-$ selectively recognizing and optically sensing bromide and iodide anions exclusively, via pure halogen bonding in aqueous methanolic solvent media (Figure 9).[19]

2.5. Molecular Modeling. The remarkable affinity of receptor 6^{2+} toward I^- and 8^{2+} toward Br^- was also investigated

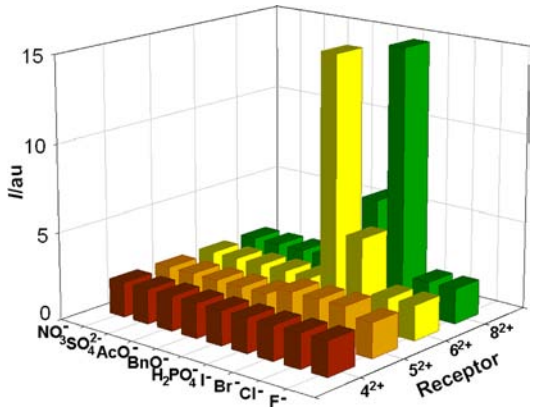

Figure 9. Graphical representation of the fluorescence emission intensity response of emission band at λ = 437 nm of receptor hexafluorophosphate salts on addition of 1 equiv of various anions in CH_3OH/H_2O 9:1 at 20 °C.

by means of Density Functional Theory (DFT) calculations and Molecular Dynamics (MD) simulations. The structures of $\mathbf{6}^{2+}$ and $\mathbf{8}^{2+}$ were optimized by DFT (Figure S17) using the B3LYP functional in methanol solution (the main component of the solvent mixture used in the binding studies) described by a polarizable continuum solvent model (see Supporting Information for full details). Since the experimental evidence suggests that XB to the receptors has a 1:1 stoichiometry in solution, the associations $\mathbf{6}\cdot Br^+$, $\mathbf{6}\cdot I^+$, $\mathbf{8}\cdot Br^+$, and $\mathbf{8}\cdot I^+$ were also optimized in the same solvent medium and are represented in Figure 10 together with relevant bond distances and angles.

In $\mathbf{6}^{2+}$, the DFT C−Br distance is 1.866 Å, while in $\mathbf{6}\cdot Br^+$ and $\mathbf{6}\cdot I^+$, the distances are slightly elongated to 1.894 and 1.881 Å. For $\mathbf{8}^{2+}$, the calculated C−I distance is 2.086 Å, while in $\mathbf{8}\cdot Br^+$ and $\mathbf{8}\cdot I^+$, they are 2.138 and 2.118 Å. The elongation of C−I upon halide interaction is also evident in the crystal structures of $\mathbf{8}^{2+}\cdot I^-\cdot PF_6^-$ and $\mathbf{8}^{2+}\cdot Br^-\cdot PF_6^-$ when the C−I covalent bond distance is compared with that found in $\mathbf{7}^{2+}$. The C−I distance in the X-ray structure of $\mathbf{8}^{2+}\cdot Br^-\cdot PF_6^-$ (2.094 Å) compares very well with the $\mathbf{8}\cdot Br^+$ value (2.138 Å) and the calculated I···Br^- distance for the C−I···Br^- halogen bond (3.192 Å) is also close to the experimental value (3.095 Å). In the X-ray structure of $\mathbf{8}^{2+}\cdot I^-\cdot PF_6^-$, the C−I distance is 2.079 Å, and the DFT one is 2.118 Å, while the I···I^- distance is also comparable (3.303 experimental vs 3.580 calculated). The agreement is not excellent but we have to take into account solid state structures correspond to a different binding scenario in which two receptor molecules are assembled by two halide anions. In contrast, in our DFT optimized structures, the receptors bind one halide using both C−X bonds in a synergetic fashion.

We calculated the Wiberg bond indexes[20] (WI), which are indicators of the bond orders and the values obtained are given in parentheses in Figure 10. The bond orders of covalent bonds C−Br in $\mathbf{6}^{2+}$ (1.100) and C−I in $\mathbf{8}^{2+}$ (1.051) are very close to 1.0, as expected for a covalent single bond. Both bond orders decrease in all receptor/halide associations, specially in $\mathbf{8}\cdot Br^+$ where the C−I bond order is reduced to 0.920 which is entirely consistent with the bond length elongation and the population of the C−I σ^* orbital. Moreover, among the C−I···Br^-, C−I···I^-, C−Br···Br^-, and C−Br···I^- XB interactions investigated, the first one in $\mathbf{8}\cdot Br^+$ has also the larger WI for the I···halide intermolecular interaction (0.161) in agreement with the experimental association constants presented in Table 3. The receptor:halide interaction energies in methanol solution at the

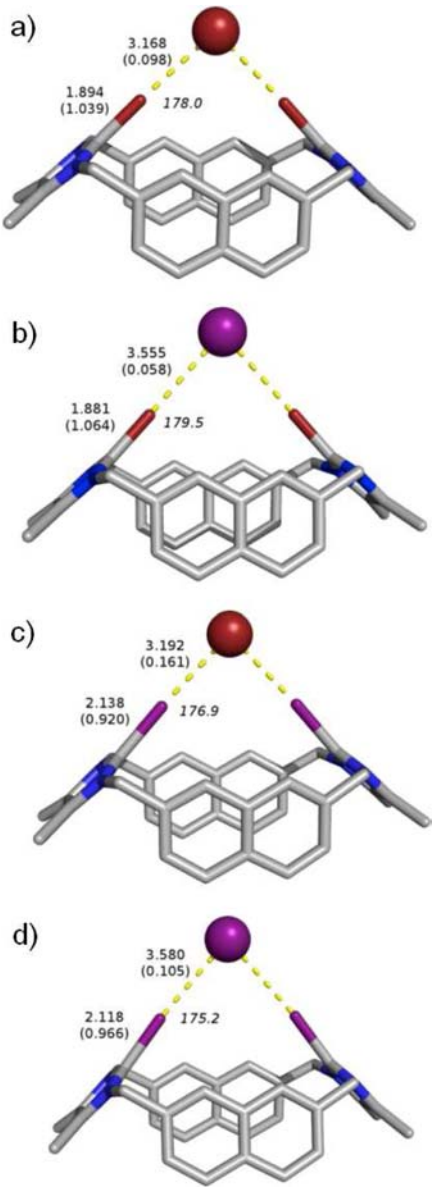

Figure 10. DFT optimized structures of $\mathbf{6}\cdot Br^+$ (a), $\mathbf{6}\cdot I^+$ (b), $\mathbf{8}\cdot Br^+$ (c), and $\mathbf{8}\cdot I^+$ (d) complexes showing the corresponding halogen bonding interactions as yellow dashed lines together with their distances (Å) and angles (°) given in italic, and Wiberg indexes in parentheses.

DFT (B3LYP) level of theory were also calculated. The results are collected in Table 4.

Table 4. Calculated (DFT, Methanol) Interaction Energies ΔE Compared with the Experimental Binding Free Energies (ΔG_{bind}) for $\mathbf{6}\cdot Br^+$, $\mathbf{6}\cdot I^+$, $\mathbf{8}\cdot Br^+$, and $\mathbf{8}\cdot I^+$ (Both Values Given in kcal mol^{-1})

complex	calculated ΔE^a	experimental $\Delta G_{bind}{}^b$
$\mathbf{6}\cdot Br^+$	−13.3	−6.0
$\mathbf{6}\cdot I^+$	−8.3	−7.8
$\mathbf{8}\cdot Br^+$	−4.3	−8.0
$\mathbf{8}\cdot I^+$	+3.5	−6.1

[a] ΔE is the difference between the energy of the complex and the energies of the isolated relaxed components. [b] ΔG_{bind} values were estimated from the experimental association constants K_a.

dx.doi.org/10.1021/ja302213r | J. Am. Chem. Soc. 2012, 134, 11533−11541

The ΔE energies for $\mathbf{6}\cdot Br^+$ and $\mathbf{6}\cdot I^+$ predict that $\mathbf{6}^{2+}$ binds bromide better than iodide while the experimental ΔG_{bind} values indicated that iodide association is slightly favored. For $\mathbf{8}^{2+}$, the results are much more acceptable since this receptor has higher affinity toward bromide as suggested by the experimental binding free energies. However, it must be mentioned that these values were calculated using a polarizable continuum model describing methanol while the experiments were performed in a 9:1 CH_3OH/H_2O solvent mixture.

The previous DFT calculations already demonstrated that $\mathbf{8}^{2+}$ is indeed able to bind bromide with great affinity in $\mathbf{8}\cdot Br^+$. Therefore, the dynamics of this interaction were further evaluated in the competitive 9:1 CH_3OH/H_2O media through molecular dynamics simulations (MD) and compared with $\mathbf{8}\cdot I^+$. Very recently, two similar approaches were proposed for the treatment of XB in MD simulations using to represent the positive region centered on the halogen atom covalently bonded (C−X), an extra-point (EP) of charge,[21] or a pseudoatom.[22] Here, we used an approach with the σ-hole represented by a dummy atom with a suitable charge located at an ideal distance of C−X (see Supporting Information for full details) which proved to be efficient for the simulation of the halogen bonding interactions between two bromo-imidazolium moieties and one chloride in a catenane assembly as described in our previous work.[11] Indeed, the use of a dummy atom allows us to describe the halogen bonding interactions of Br^- and I^- with $\mathbf{8}^{2+}$, as evident in molecular mechanics (MM) minimized structures of these associations shown in Supporting Information. Subsequently, those MM minimized structures were immersed in cubic boxes of a 9:1 CH_3OH/H_2O mixture (~40 Å side, after equilibration period) and MD simulations were performed with AMBER11[23] with parameters from the General AMBER Force Field[24] and using the pmemd.cuda AMBER executable, able to accelerate explicit solvent Particle Mesh Ewald (PME) calculations through the use of GPUs.[25] The structural data were collected along 30 ns preceded by a multistage equilibration protocol described in Supporting Information. Representative snapshots of $\mathbf{8}\cdot Br^+$ and $\mathbf{8}\cdot I^+$ associations in solution are depicted in Figure 11.

The two simultaneous C−I···halide halogen bonds observed in the structures of $\mathbf{8}\cdot Br^+$ and $\mathbf{8}\cdot I^+$ are preserved during the entire time of the long collection period (see Supporting Information, Figure S19). In $\mathbf{8}\cdot Br^+$ the I···Br^- distances fluctuate around 3.5 Å, with averages of 3.553 ± 0.139 Å and 3.548 ± 0.139 Å, which are large when compared with the DFT values (3.192 Å). However, it must be pointed out that the DFT optimization was conducted in the methanol solvent continuum model while the MD simulations were performed in 9:1 CH_3OH/H_2O mixture with the dummy atom approximation to enable the XB interaction. Therefore, in these circumstances, the results obtained are quite acceptable. For $\mathbf{8}\cdot I^+$, the I···I^- distances fluctuate around 3.7 Å, with averages of 3.7842 ± 0.1566 Å and 3.7863 ± 0.1583 Å, closer to the DFT values (3.580 Å).

Our MD simulations clearly demonstrate that the $\mathbf{8}\cdot Br^+$ association, through the two cooperative XB interactions, is stable during the simulation time even in a competitive media such as a CH_3OH/H_2O (9:1) solution. The $\mathbf{8}\cdot I^+$ association is also maintained in agreement with the large experimental binding constant (3.71×10^4 M^{-1}).

The solvation of $\mathbf{8}\cdot Br^+$ and $\mathbf{8}\cdot I^+$ associations by methanol and water solvent molecules was also evaluated from MD data. Figure 12 depicts the individual radial distribution function,

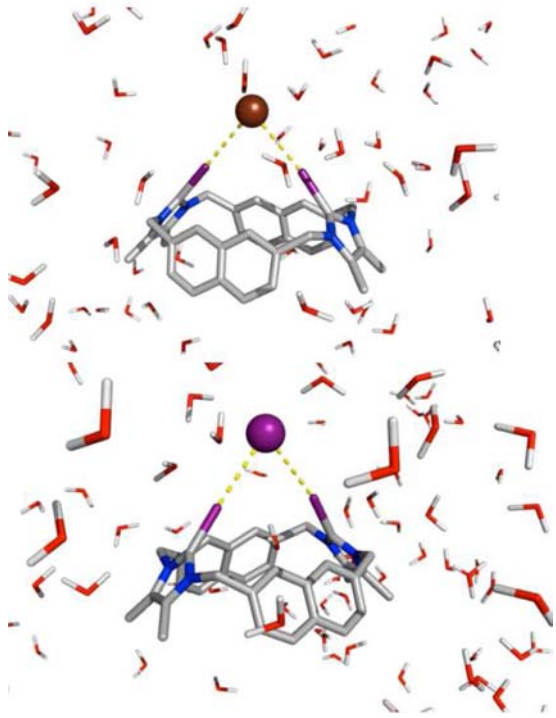

Figure 11. Representative snapshots of $\mathbf{8}\cdot Br^+$ (top), $\mathbf{8}\cdot I^+$ (bottom) in CH_3OH/H_2O (9:1) solution showing both associations surrounded by water molecules. Methanol molecules and the receptor hydrogen atoms were omitted for clarity. Halogen-bonds are represented as yellow dashed lines.

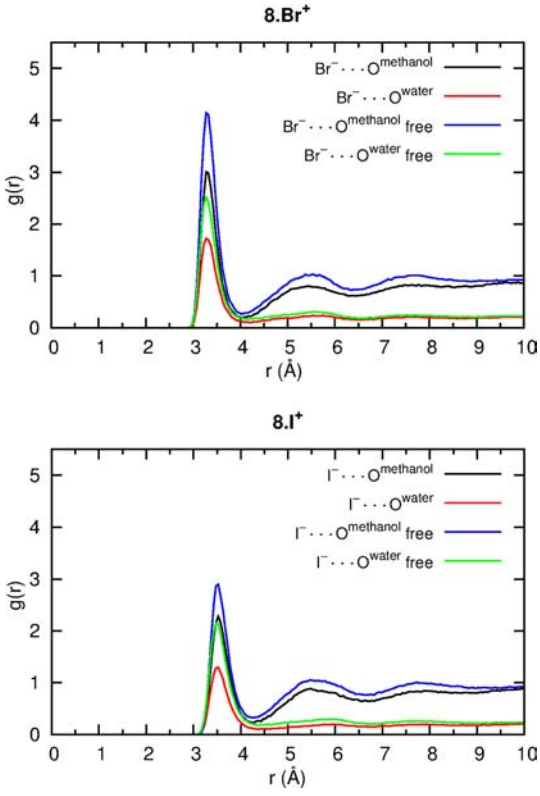

Figure 12. RDFs of methanol and water oxygen atoms around bromide ($\mathbf{8}\cdot Br^+$, top) and iodide ($\mathbf{8}\cdot I^+$, bottom) compared with the free anions in the same solution.

dx.doi.org/10.1021/ja302213r | J. Am. Chem. Soc. 2012, 134, 11533−11541

RDF $g(r)$ of both solvent molecule around the bromide (top) and iodide (bottom) in $\mathbf{8}\cdot Br^+$and in $\mathbf{8}\cdot I^+$ associations, respectively. For comparison purposes, MD simulations with a free bromide and iodide anions were also carried out in the same conditions and the corresponding RDFs are also shown in the same plot.

The first solvent shell for methanol and water molecules around bromide in $\mathbf{8}\cdot Br^+$ occurs as well-defined peaks centered at ~3.4 Å. As would be expected, the density of methanol molecules is larger than that of water. A second solvation sphere for methanol and water (with less intensity) appears at ~5.5 Å. When compared with the free bromide RDF, it is evident that the density of both solvent molecules around the anion decreases in the presence of receptor $\mathbf{8}^{2+}$, but the water and methanol peak positions are not affected by the receptor. For $\mathbf{8}\cdot I^+$, the scenario is equivalent although the difference from the free iodide peaks and the complexed ones in $\mathbf{8}\cdot I^+$ is much less pronounced meaning that the receptor has a lower impact on the solvation of the I^- anion.

All the above results, DFT calculations plus MD simulations, demonstrate that indeed, $\mathbf{8}\cdot Br^+$ is a stable association in the presence of water. $\mathbf{8}\cdot I^+$ should also be stable, although relatively less so than $\mathbf{8}\cdot Br^+$.

3. CONCLUSION

The synthesis of a new family of fluorescent XB macrocyclic halo-imidazolium receptors has been achieved where chloro-, bromo-, and iodo-imidazolium motifs are integrated into a cyclic molecular framework using naphthalene spacer groups. The large size of the iodine atom substituents were found to inhibit intramolecular ring rotation resulting in the isolation of anti and syn conformers of the iodo-imidazoliophane, whereas the chloro- and bromo-imidazoliophane analogues exhibit solution dynamic conformational properties on the NMR time scale. X-ray structural analysis revealed the syn iodo-imidazoliophane isomer $\mathbf{8}^{2+}$ to form novel dimeric isostructural XB complexes of 2:2 stoichiometry with bromide and iodide anions in the solid state. Solution phase DOSY NMR experiments, however, suggest iodide recognition takes place via cooperative convergent XB–iodide 1:1 stoichiometric binding in aqueous solvent mixtures. ^{1}H NMR and fluorescence spectroscopic titration experiments with a variety of anions in the competitive CD_3OD/D_2O (9:1) aqueous solvent mixture demonstrated the bromo- $\mathbf{6}^{2+}$ and syn iodo-imidazoliophane isomer $\mathbf{8}^{2+}$ to exhibit remarkably strong and selective XB recognition of iodide and bromide anions, respectively. Importantly, $\mathbf{6}^{2+}$ and $\mathbf{8}^{2+}$ are capable of optically sensing these halide anions *exclusively* via a fluorescence response and, to the best of our knowledge, represent the first examples of XB chemosensors to function in aqueous solvent mixtures. In stark contrast, no evidence of anion sensing was observed with protic-, chloro-, and anti iodo-imidazoliophane receptors in this aqueous methanolic solvent mixture. Computational DFT and molecular dynamics simulations corroborate the experimental observations that receptors $\mathbf{6}^{2+}$ and $\mathbf{8}^{2+}$ form stable cooperative convergent XB associations with bromide and iodide in aqueous methanolic media.

■ ASSOCIATED CONTENT

Supporting Information

Experimental procedures and spectroscopic data for all new compounds, full crystallographic and computational details are available. This material is available free of charge via the Internet at http://pubs.acs.org.

■ AUTHOR INFORMATION

Corresponding Author

paul.beer@chem.ox.ac.uk

Notes

The authors declare no competing financial interest.

■ ACKNOWLEDGMENTS

F.Z. acknowledges Ministry of Education of Spain for a Postdoctoral contract (Programa Nacional de Movilidad de Recursos Humanos del Plan Nacional I+D+I 2008-2011). A.C. acknowledges the European Union for a Marie Curie Postdoctoral Fellowship. N.G.W. acknowledges Clarendon Fund and Trinity College for a studentship. P.J.C. thanks FCT for the postdoctoral grant SFRH/BPD/27082/2006. We acknowledge Oxford University Crystallography Service for instrument use.

■ REFERENCES

(1) (a) Beer, P. D.; Gale, P. A. *Angew. Chem., Int. Ed.* **2001**, *40*, 486–512. (b) O'Neil, E. J.; Smith, B. D. *Coord. Chem. Rev.* **2006**, *250*, 3068–3080. (c) Sessler, J. L.; Gale, P. A.; Cho, W.-S. *Anion Receptor Chemistry*; RSC: Cambridge, 2006; (d) Llinares, J. M.; Powell, D.; Bowman-James, K. *Coord. Chem. Rev.* **2003**, *240*, 57–75. (e) Martínez-Mañez, R.; Sancenón, F. *Coord. Chem. Rev.* **2006**, *250*, 3081–3093. (f) Gunnlaugsson, T.; Glynn, M.; Tocci, G. M.; Kruger, P. E.; Pfeffer, F. M. *Coord. Chem. Rev.* **2006**, *250*, 3094–3117. (g) Rice, C. R. *Coord. Chem. Rev.* **2006**, *250*, 3190. (h) Gale, P. A; García-Garrido, S. E.; Garric, J. *Chem. Soc. Rev.* **2008**, *37*, 151–190. (i) Pérez, J.; Riera, L. *Chem. Soc. Rev.* **2008**, *37*, 2658–2667. (j) Steed, J. W. *Chem. Soc. Rev.* **2009**, *38*, 506–519. (k) Kubik, S. *Chem. Soc. Rev.* **2009**, *38*, 585–605. (l) Hua, Y.; Flood, A. H. *Chem. Soc. Rev.* **2010**, *39*, 1262–1271.

(2) (a) Pierangelo, M.; Franck, M.; Tullio, P.; Giuseppe, R.; Giancarlo, T. *Angew. Chem., Int. Ed.* **2008**, *47*, 6114–6127. (b) Hudnall, T. W.; Chiu, C.-W.; Gabbaï, F. P. *Acc. Chem. Res.* **2009**, *42*, 388–397.

(3) (a) Gamez, P.; Mooibroek, T. J.; Teat, S. J.; Reedijk, J. *Acc. Chem. Res.* **2007**, *40*, 435–444. (b) Hay, B. P.; Bryantsev, V. S. *Chem. Commun.* **2008**, 2417–2428. (c) Schottel, B. L.; Chifotides, H. T.; Dunbar, K. R. *Chem. Soc. Rev.* **2008**, *37*, 68–83. (d) Rosokha, V.; S. Lindeman, V.; Rosokha, S. V.; Kochi, J. K. *Angew. Chem., Int. Ed.* **2004**, *43*, 4650–4652. (e) Berryman, O. B.; Hof, F.; Hynes, M. J.; Johnson, D. W. *Chem. Commun.* **2006**, 506–508.

(4) (a) Metrangolo, P.; Meyer, F.; Pilati, T.; Resnati, G.; Terraneo, G. *Angew. Chem., Int. Ed.* **2008**, *47*, 6114–6127. (b) Metrangolo, P.; Neukirch, H.; Pilati, T.; Resnati, G. *Acc. Chem. Res.* **2005**, *38*, 386–395. (c) Politzer, P.; Lane, P.; Concha, M. C.; Ma, Y.; Murray, J. S. *J. Mol. Model.* **2007**, *13*, 305–311.

(5) Rissanen, K. *Cryst. Eng. Commun.* **2008**, *10*, 1107–1113.

(6) (a) Metrangolo, P.; Prasang, C.; Resnati, G.; Liantonio, R.; Whitwood, A. C.; Bruce, D. W. *Chem. Commun.* **2006**, 3290–3292. (b) Cincic, D.; Friscic, T.; Jones, W. *Chem.–Eur. J.* **2008**, *14*, 747–753. (c) Metrangolo, P.; Meyer, F.; Pilati, T.; Proserpio, D. M.; Resnati, G. *Cryst. Growth Des.* **2008**, *8*, 654–659. (d) Xu, J. W.; Liu, X. M.; Ng, J. K. P.; Lin, T. T.; He, C. B. *J. Mater. Chem.* **2006**, *16*, 3540–3595. (e) Bruce, D. W.; Metrangolo, P.; Meyer, F.; Prasang, C.; Resnati, G.; Terraneo, G.; Whitwood, A. C. *New J. Chem.* **2008**, *32*, 477–482. (f) Zordan, F.; Brammer, L.; Sherwood, P. *J. Am. Chem. Soc.* **2005**, *127*, 5979–5989. (g) Fourmigué, M.; Batail, P. *Chem. Rev.* **2004**, *104*, 5379–5418. (h) Liantonio, R.; Metrangolo, P.; Meyer, F.; Pilati, T.; Navarrini, W.; Resnati, G. *Chem. Commun.* **2006**, 1819–1821. (i) Graeme, R. H.; Paul, J.; John, M.; Llew, R.; Aaron, S. M. *Chem.—Eur. J.* **2009**, *15*, 4156–4164. (j) Präsang, C.; Nguyen, H. L.; Horton, P. N.; Whitwood, A. C.; Bruce, D. W. *Chem. Commun.* **2008**, 6164–6166. (k) Bruce, D. W. *Halogen Bonding: Fundamentals and*

Applications; Metrangolo, P., Resnati, G., Eds.; Springer: Berlin, 2008; Vol. *126*, p 161; (l) Fourmigue, M. *Halogen Bonding: Fundamentals and Applications*; Metrangolo, P., Resnati, G., Eds.; Springer: Berlin, 2008; Vol. *126*, p 181.

(7) (a) Reid, C.; Mulliken, R. S. *J. Am. Chem. Soc.* **1954**, *76*, 3869. (b) Larsen, D. W.; Allred, A. L. *J. Am. Chem. Soc.* **1965**, *87*, 1216–1219. (c) Larsen, D. W.; Allred, A. L. *J. Phys. Chem.* **1965**, *69*, 2400–2401. (d) Messina, M. T.; Metrangolo, P.; Panrezi, W.; Ragg, E.; Resnati, G. *Tetrahedron Lett.* **1998**, *39*, 9096–9072. (e) Metrangolo, P.; Panrezi, W.; Recupero, F.; Resnati, G. *J. Fluorine Chem.* **2002**, *114*, 27–33. (f) Libri, S.; Jasim, N. A.; Perutz, R. N.; Brammer, L. *J. Am. Chem. Soc.* **2008**, *130*, 7842–7844. (g) Cabot, R.; Hunter, C. A. *Chem. Commun.* **2009**, 2005–2007. (h) Derossi, S.; Brammer, L.; Hunter, C. A.; Ward, M. D. *Inorg. Chem.* **2009**, *48*, 1666–1677. (i) Beweries, T.; Brammer, L.; Jasim, N. A.; McGrady, J. E.; Perutz, R. N.; Whitwood, A. C. *J. Am. Chem. Soc.* **2011**, *133*, 14338–14348. (j) Yunxiang, L.; Ting, S.; Yong, W.; Huaiyu, Y.; Xiuhua, Y.; Xiaoming, L.; Hualiang, J.; Weiliang, Z. *J. Med. Chem.* **2009**, *52*, 2854–2862. (k) Hardegger, L. A.; Kuhn, B.; Spinnler, B.; Anselm, L.; Ecabert, R.; Stihle, M.; Gsell, B.; Thoma, R.; Diez, J.; Benz, J.; Plancher, J.-M.; Hartmann, G.; Banner, D. W.; Haap, W.; Diederich, F. *Angew. Chem., Int. Ed.* **2011**, *50*, 314–318. (l) Bruckmann, A.; Pena, M. A.; Bolm, C. *Synlett* **2008**, 900. (m) Kraut, D. A.; Churchill, M. J.; E. Dawson, P.; Herschlag, D. *ACS Chem. Biol.* **2009**, *4*, 269–273. (n) Walter, S. M.; Kniep, F.; Herdtweck, E.; Huber, S. M. *Angew. Chem., Int. Ed.* **2011**, *50*, 7187–7191. (o) Dordonne, S.; Crousse, B.; Bonnet-Delpon, D.; Legros, J. *Chem. Commun.* **2011**, *47*, 5855–5857. (p) Walter, S. M.; Kniep, F.; Herdtweck, E.; Huber, S. M. *Angew. Chem., Int. Ed.* **2011**, *50*, 7187–7191. (q) Laurence, C.; Graton, J.; Berthelot, M.; El Ghomari, M. J. *Chem.—Eur. J.* **2011**, *17*, 10431–10444. (r) Carlsson, A. C. C.; Grafenstein, J.; Laurila, J. L.; Bergquist, J.; Erdelyi, M. *Chem. Commun.* **2011**, *48*, 1458–1460. (s) Erdelyi, M. *Chem. Soc. Rev.* **2012**, *41*, 3547–3557.

(8) (a) Caballero, A.; White, N. G.; Beer, P. D. *Angew. Chem., Int. Ed.* **2011**, *50*, 1845–1848. (b) Sarwar, M. G.; Dragisic, B.; Salsberg, L. J.; Gouliaras, C.; Taylor, M. S. *J. Am. Chem. Soc.* **2010**, *132*, 1646–1653. (c) Sarwar, M. G.; Dragisic, B.; Sagoo, S.; Taylor, M. S. *Angew. Chem., Int. Ed.* **2010**, *49*, 1674–1677. (d) Chudzinski, M. G.; McClary, C. A.; Taylor, M. S. *J. Am. Chem. Soc.* **2011**, *133*, 10559–10567. (e) Mele, A.; Metrangolo, P.; Neukirch, H.; Pilati, T.; Resnati, G. *J. Am. Chem. Soc.* **2005**, *127*, 14972–14973. (f) Dimitrijević, E.; Kvak, O.; Taylor, M. S. *Chem. Commun.* **2010**, *46*, 9025–9027. (g) Kilah, N. L.; Wise, M. D.; Beer, P. D. *Cryst. Growth Des.* **2011**, *11*, 4565–4571. (h) Cametti, M.; Raatikainen, K.; Metrangolo, P.; Pilati, T.; Terraneo, G.; Resnati, G. *Org. Biomol. Chem.* **2012**, *10*, 1329–1333. (i) Jentzsch, A. V.; Emery, D.; Mareda, J.; Metrangolo, P.; Resnati, G.; Matile, S. *Angew. Chem., Int. Ed.* **2011**, *50*, 11675–11678.

(9) Chudzinski, M. G.; McClary, C. A.; Taylor, M. S. *J. Am. Chem. Soc.* **2011**, *133*, 10559–10567.

(10) Kilah, N. L.; Wise, M. D.; Serpell, C. J.; Thompson, A. L.; White, N. G.; Christensen, K. E.; Beer, P. D. *J. Am. Chem. Soc.* **2010**, *132*, 11893–11895.

(11) A halogen bonding catenane has recently been shown to sense via fluorescence chloride and bromide in acetonitrile solution: Caballero, A.; Zapata, F.; White, N. G.; Costa, P. J.; Felix, V.; Beer, P. D. *Angew. Chem., Int. Ed.* **2012**, *51*, 1876–1880.

(12) Baker, M. V.; Brown, D. H.; Heath, C. H.; Skelton, B. W.; White, A. H.; Williams, C. C. *J. Org. Chem.* **2008**, *73*, 9340–9352.

(13) Sandström, J. *Dynamic NMR Spectroscopy*; Academic Press: London, 1982.

(14) Lu, Y.-X.; Zou, J.-W.; Wang, Y.-H.; Jiang, Y.-J.; Yu, Q.-S. *J. Phys. Chem. A.* **2007**, *111*, 10781–10788.

(15) Hynes, M. J. *J. Chem. Soc., Dalton Trans.* **1993**, 311–312.

(16) Undertaking analogous DOSY NMR experiments in CD_3OD/D_2O 9:1 resulted in complex precipitation.

(17) Analogous ^1H NMR titrations experiments in CD_3CN revealed receptor $\mathbf{4}^{2+}\cdot 2PF_6^-$ to bind chloride the most strongly (see Supporting Information). This suggests competitive solvation effects are responsible for chloride being weakly complexed in the aqueous methanolic solvent mixture (CD_3OD:D_2O 9:1).

(18) *SPECFIT*, 2.02; Spectrum Software Associates: Chapel Hill, NC.

(19) Both $\mathbf{6}^{2+}\cdot 2PF_6^-$ and $\mathbf{8}^{2+}\cdot 2PF_6^-$ XB receptors are significantly superior bromide and iodide anion complexing agents in comparison to the previously reported bromo-imidazoliophane xylene system (see ref 8a).

(20) Wiberg, K. B. *Tetrahedron* **1968**, *24*, 1083.

(21) Ibrahim, M. A. A. *J. Comput. Chem.* **2011**, *32*, 2564–2574.

(22) Rendine, S.; Pieraccini, S.; Forni, A; Sironi, M. *Phys. Chem. Chem. Phys.* **2011**, *13*, 19508–19516.

(23) Case, D. A.; Darden, T. A.; Cheatham, T. E., I; Simmerling, C. L.; Wang, J.; Duke, R. E.; Luo, R.; Crowley, M.; Walker, R. C.; Zhang, W.; Merz, K. M.; Wang, B.; Hayik, S.; Roitberg, A.; Seabra, G.; Kolossvary, I.; Wong, K. F.; Paesani, F.; Vanicek, J.; Wu, X.; Brozell, S. R.; Steinbrecher, T.; Gohlke, H.; Yang, L.; Tan, C.; Mongan, J.; Hornak, V.; Cui, G.; Mathews, D. H.; Seetin, M. G.; Sagui, C.; Babin, V.; Kollman, P. A. *AMBER11*, University of California: San Francisco, 2010.

(24) Wang, J.; R. Wolf, M.; Caldwell, J. W.; Kollman, P. A.; Case, D. A. *J. Comput. Chem.* **2004**, *25*, 1157–1174.

(25) (a) See AMBER 12 NVIDIA GPU Acceleration Support Home Page. http://ambermd.org/gpus/ (accessed in 2011/11/03).